Electronic Supplementary Material (ESI) for Nanoscale.

Supporting Materials

High-Mobility Anisotropic Transport in Few-layer γ-B_{28} Films

Liangzhi Kou[1, 2,*], Yandong Ma[3], Liujiang Zhu[4], Ziqi Sun[1], Yuantong Gu[1], Aijun Du[1], Sean Smith[2], Changfeng Chen[5]

[1] *School of Chemistry, Physics and Mechanical Engineering Faculty, Queensland University of Technology, Garden Point Campus, QLD 4001, Brisbane, Australia*

2 Integrated Materials Design Centre (IMDC), School of Chemical Engineering, University of New South Wales, Sydney, New South Wales 2052, Australia

3 Engineering and Science, Jacobs University Bremen, Campus Ring 1, 28759 Bremen, Germany

4 Bremen Center for Computational Materials Science, University of Bremen, Am Falturm 1, 28359 Bremen, Germany

[5] *Department of Physics and Astronomy and High Pressure Science and Engineering Center, University of Nevada, Las Vegas, Nevada 89154, United States*

Computational Methods

Structural relaxation and electronic calculations were carried out by first-principles calculations based on the density functional theory (DFT) as implemented in the Vienna Ab Initio Simulation (VASP) package.[s1] The exchange correlation interaction was treated within the generalized gradient approximation (GGA).[s2] The structural models for γ-B_{28} films are periodic in the xy plane and separated by at least 10 Å along the z direction to avoid the interactions between adjacent layers. All of the atoms in the unit cell are fully relaxed until the force on each atom is less than 0.01 eV/Å. The Brillouin zone integration was sampled by a 10 × 8 × 1 k-grid mesh for a unit cell. An energy cutoff of 400 eV was chosen for the plane wave basis. The vdW interaction is introduced, and it is described by a semiempirical correction by the Grimme method.[s3] We also employed the Heyd-Scuseria-Ernzerhof (HSE) [s4] hybrid functional in calculating the electronic band structure. HSE employs a screened short-range Hartree-Fock exchange instead of the full exact exchange, thus drastically reducing the computational requirements and, at the same time, overcoming the known problems of the Hartree-Fock exchange. We take the mixing parameter for the short-range exchange as 0.25, while K points and energy cutoff are the same as above PBE calculation.

The carrier mobility (μ) is calculated based on the deformation theory proposed by Bardeen and Shockley,[s5] For inorganic semiconductors, the coherent wavelength of thermally activated electrons or holes is close to the acoustic phonon wavelength and is much longer than typical bond length; therefore, the scattering of a thermal electron or hole is dominated by the electron-acoustic phonon coupling.[25] On the basis of effective mass approximation, the charge mobility in 2D materials can be expressed as:

$$\mu = \frac{2e\hbar^3 C}{3k_B T|m^*|^2 E_1^2} \quad [1]$$

Here, C is the elastic modulus defined as $C = \frac{\partial^2 E}{\partial \epsilon^2}/S_0$, E is the total energy, ϵ is the uniaxial strain, S_0 is the area of the optimized γ-B_{28} film, T is the temperature, and E_1 is the deformation potential constant, which is proportional to the band edge shift induced by the strain. E_1 is defined as $\Delta E = E_1 \epsilon$ where ΔE is the energy shift of the band edge position with respect to strain ϵ along the direction a or b.

Strain Effect on the Electronic Band Structure of Four-layer γ-B_{28} Film

Using the methods presented above, we have performed calculations to check the effect of structural deformation on the surface states and pseudogap in the four-layer γ-B_{28} films by applying a uniaxial strain defined as $\epsilon = \Delta l / l_0$, where l_0 is equilibrium lattice constant (*a* or *b*) and Δl is its variation. The results of the band gap modulation by strain under compressive and tensile strain are shown in Fig. s0 (a). It is noted that all the band gap opening and closure happen at the surface while the electronic band structure of the interior layers is only slightly affected by strain, namely, the electronic modulation under strain is not uniform throughout the film. This is because the electronic states and the associated pseudogap modulation near the Fermi level are dominated by the states from the surface layer as shown in Fig. 3 in the main text. The surface states from the VBM and CBM touch each other at the Γ point, forming the metallic surface states as in 3D TIs at strain of 0.5% along the *b* direction or -1% along the *a* direction. Under a biaxial tensile strain, the metallic surface states are preserved. This is because the conduction and valence band edge states are shifted to the Γ-X direction induced by the Brillouin zone distortion under the biaxial tension; the system remains in metallic state despite a gap opening between the conduction and valence states at the Γ point (see Fig. s3 below). Another notable feature is the anisotropy of the strain modulated electronic properties. The pseudogap variation as a function of strain along the *b* direction is much more significant than that along the *a* direction. For example, at 5% strain along the *b* direction, the surface pseudogap is opened to 230 meV; while it is only 97 meV along the *a* direction at the same strain level.

To determine the carrier mobility, we also examined the 2D elastic modulus (C) and the deformation-potential constant (E_1) of the four-layer γ-B_{28} film. We have varied the lattice constant in the ±1 % range along both the *a* and *b* directions to calculate the response of the total energy [Fig. s0 (b)] and the shift of the positions of the conduction band and valance band [Fig. s0 (c); although conduction band crosses Fermi level due to electrostatic potential difference, we regard it as CBM while the adjacent below one as VBM) as a function of strain. The calculated results show that the band state variation in response to strain is highly anisotropic. The VBM increases monotonously with strain along both directions, whereas the

CBM decreases monotonously with strain along the *a* direction but increases slightly along the *b* direction. The 2D elastic modulus (C) is obtained by a quadratic fitting of the total energy versus strain curves, and the deformation potential constant (E_1) is calculated by the linear fitting of the CBM (VBM)–strain relation. The 2D modulus along the *b* direction is larger than that along the *a* direction because the B-B bonding strength along the *a* direction is weaker than that along the *b* direction. The B-B bond length between B_{12} and B_2 in bulk γ-B_{28} is 2.07 Å along the *a* axis and 1.65 Å along the *b* axis as shown in Fig. 1a in the main text, while the corresponding values in films thicker than trilayer are essentially the same. The difference between the B-B bonding strength along the two directions renders the deformation-potential constant along the *b* direction being larger than that along the *a* direction, while the band energy is more sensitive to strain along the *b* direction than along the *a* direction.

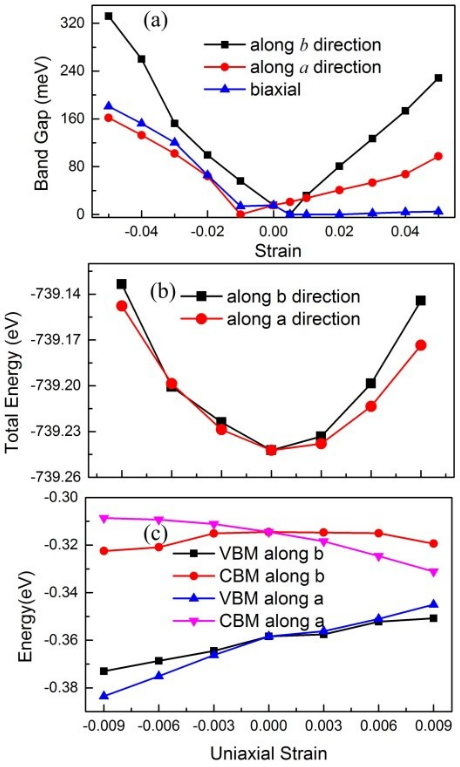

Figure s0. (a) The pseudogap, (b) total energy, and (c) band edge shift versus strain for the four-layer γ-B_{28} film.

References

[s1] G. Kresse, J. Furthmüller, *Phys. Rev. B* **1996**, *54*, 11169-11186.

[s2] J. P. Perdew, K. Burke, M. Ernzerhof, *Phys. Rev. Lett.* **1996**, *77*, 3865-3868.
[s3] S. Grimme, *J. Comp. Chem.* **2006**, *27*, 1787-1799.
[s4] J. Heyd, G. E. Scuseria, and M. Ernzerhof, J. Chem. Phys. **2003**, 118, 8207
[s5] J. Bardeen, W. Shockley, *Phys. Rev.* **1950**, *80*, 72-80.

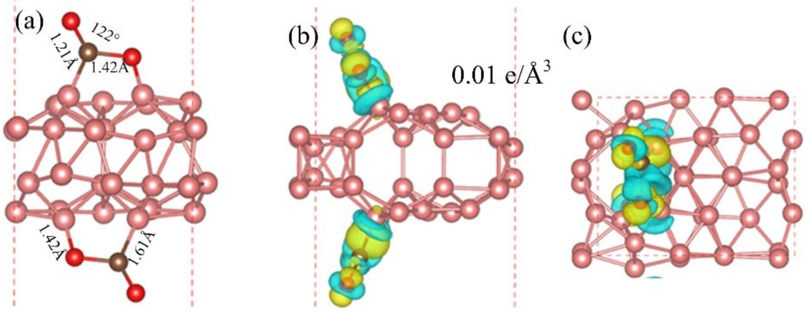

Figure s1. (a) The adsorption configuration of CO_2 on γ-B_{28} layer; (b, c) electron transfer after CO_2 absorption on γ-B_{28} layer.

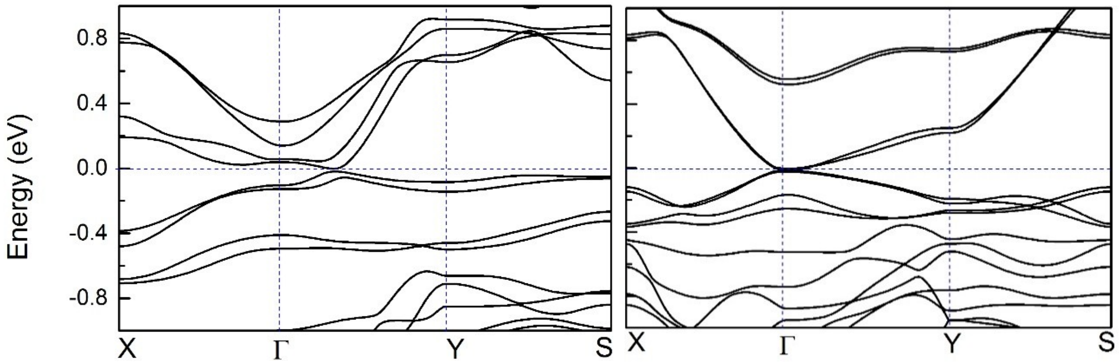

Figure s2. Bandstructures of 3(left) and 4 (right) layer γ-B_{28} layers with 2 electrons removed from system, the Fermi level is located in the band gap, they are semiconductors with gap of 98 and 15.4 meV, respectively. Fermi level is indicated with dashed blue lines.

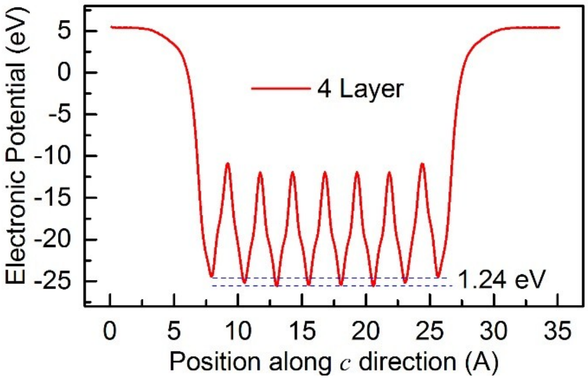

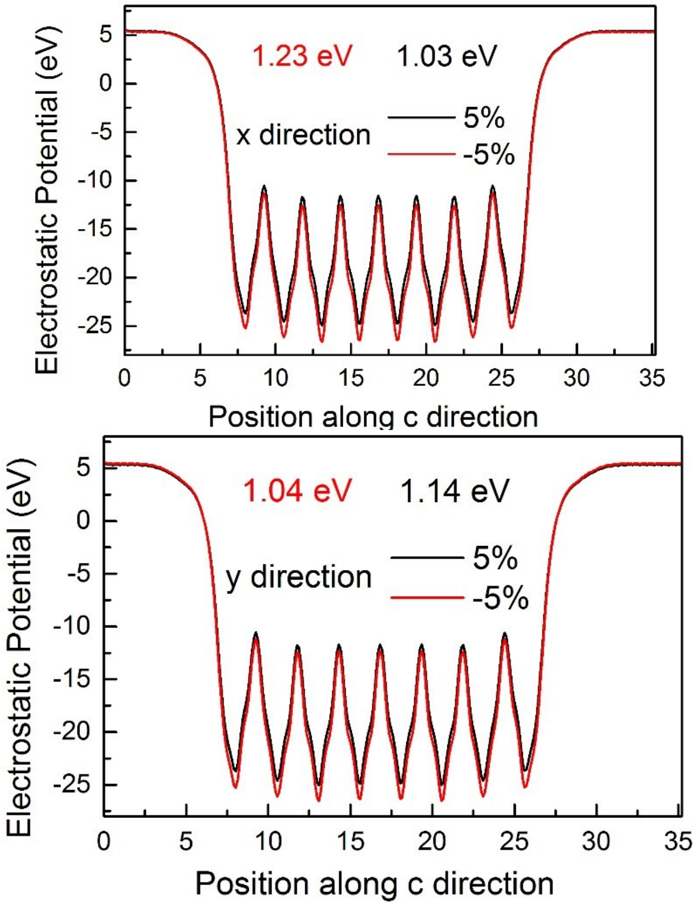

Figure s3. The calculated electrostatic potential along the thickness direction of a four-layer γ-B_{28} film under strain of 0% (upper), ±5% along x direction (middle) and y direction (below).

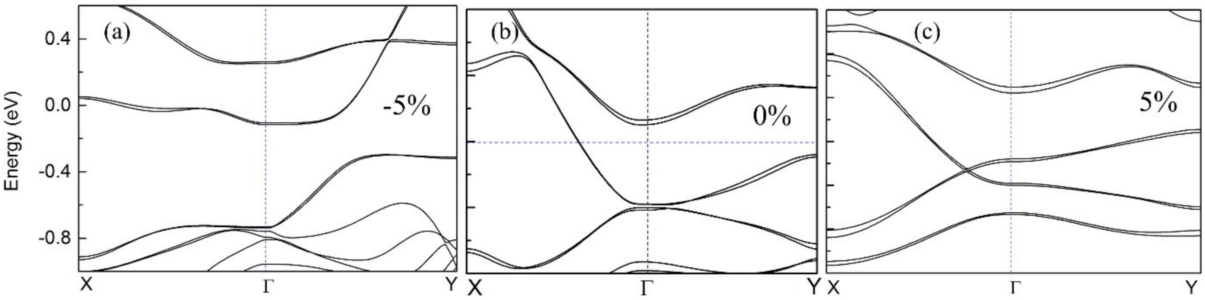

Figure s4. Electronic properties of four-layer of γ-B_{28} under strain of -5%, 0% and 5%. When 2 electrons are removed from the system, the Fermi level will be shifted to middle of gap.

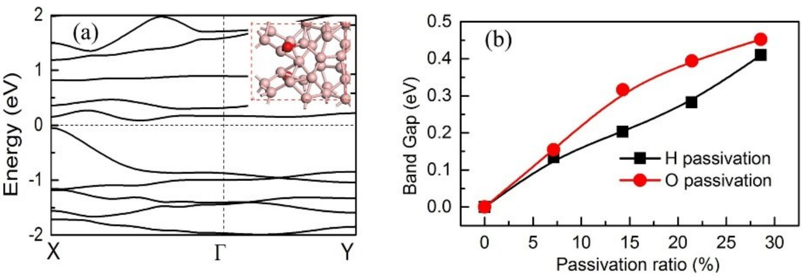

Figure s5. (a) Electronic band structure of monolayer γ-B_{28} with one oxygen atom adsorption on each surface of the unit cell (see inset); (b) bandgap variation versus the oxygen or hydrogen passivation rate (defined as $n_H(n_O)/n_B \times 100\%$, where n_X is the number of X atom).

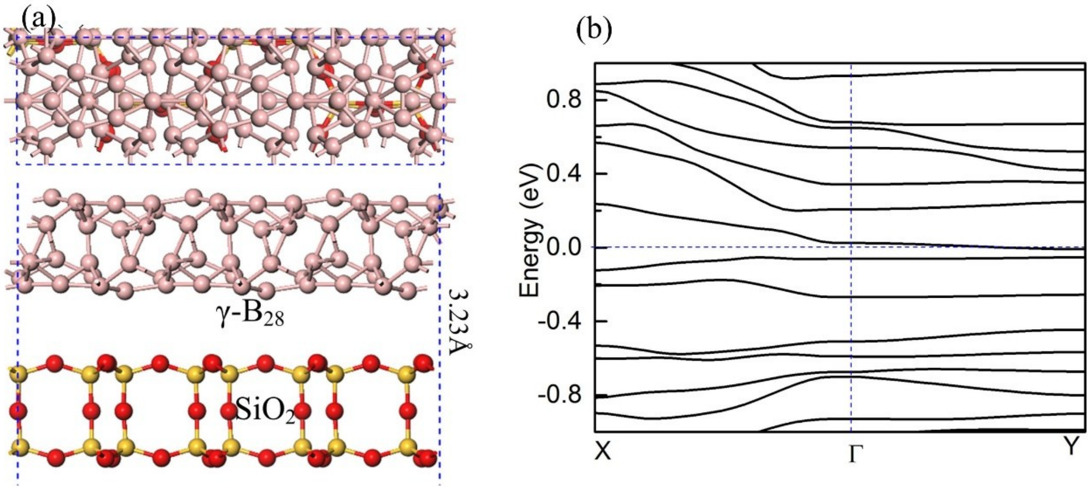

Figure s6. (a) Top and side view of the fully relaxed structures of monolayer γ-B_{28} on SiO_2 substrate, and (b) the corresponding electronic band structure.

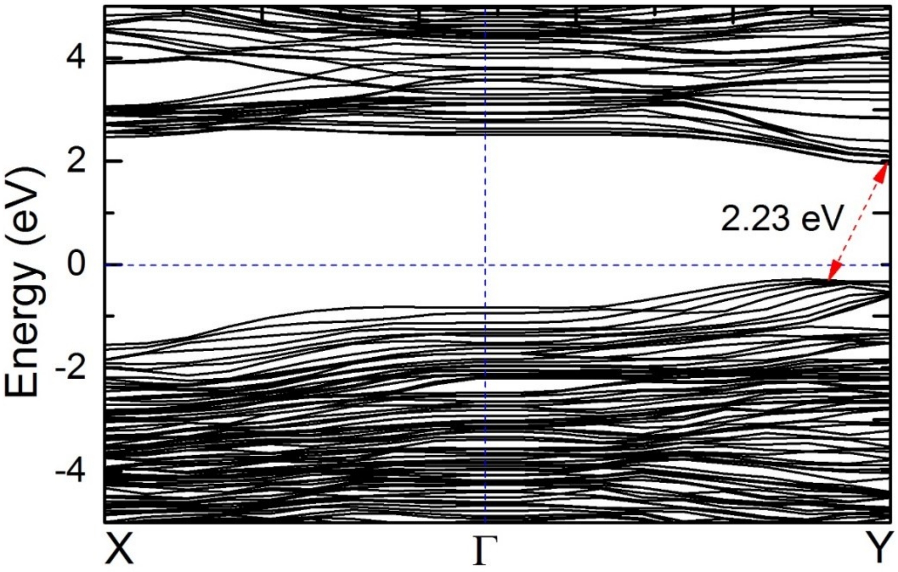

Figure s7. Band structure of the 4-layer B&H passivated γ-B_{28} from HSE06 calculations, which produce an indirect band gap of 2.23 eV.